Available online at www.sciencedirect.com

SCIENCE DIRECT®

Inorganica Chimica Acta 359 (2006) 3105–3110

Inorganica Chimica Acta

www.elsevier.com/locate/ica

Synthesis, characterization and crystal structure of manganese (IV) complex derived from salicylic acid

Ram A. Lal [a,*], Samhita Bhaumik [b], Aka Lemtur [a], Mahesh K. Singh [b], Debjani Basumatari [a], Sanjesh Choudhury [a], Arjun De [b], Arvind Kumar [c]

[a] *Department of Chemistry, North-Eastern Hill University, Shillong 793022, Meghalaya, India*
[b] *Department of Chemistry, Tripura University, Suryamaninagar 799130, Tripura, India*
[c] *Department of Chemistry, Rice University, 1600 Main Street, MS-60, Houston, TX 77005, USA*

Received 20 May 2004; received in revised form 19 November 2004; accepted 28 November 2004

Abstract

The binuclear manganese (IV) $[Mn_2(Hsal)_4(OH)_4]$ (H_2sal = salicylic acid) complex has been obtained from a complex reaction mixture in methanol consisting of $Mn(II)(OAc)_2 \cdot 4H_2O$, GS (a reagent obtained by refluxing glycine and salicylaldehyde in 1:1 molar ratio in methanol), monosodium salicylate and pyridine. The compound contains a distorted octahedral MnO_6 coordination unit of potential importance to high oxidation state manganese bimolecules.

Keywords: Maganese (IV) complex; Salicylic acid; Crystal structure; Spectroscopic data

1. Introduction

The chemistry of manganese is the subject of much current interest owing to its involvement in a number of biological systems, e.g., superoxide dismutase [1] and an azide sensitive catalase [2]. The role of manganese in the oxygen evolving complex (OEC) of photosystem II (PS II) is of great importance [3–8]. Manganese appears to serve as an electron transfer agent in the charge accumulation center of the water oxidizing system in reaction with PS II. It is proposed that in PS II, manganese functions as template to bring the oxygen atoms of two water molecules into close proximity to form an O–O bond [9]. Quinones are not effective ligands for transition metal ions, although they are present in significant quantities in chloroplasts. A model for the manganese cofactor of photosystem II has been prepared that makes use of manganese catechol complexes as template for the preparation of O–O bond.

It is essential that four manganese ions are necessary for high rates of oxygen evolution [10]. It has been shown by EXAFS studies and further by XANES studies that these four ions are arranged in two [11] or perhaps three [12] in equivalent binuclear environments with two distinct Mn···Mn separations. Manganese atoms in one set are separated by a short distance of ca. 2.7 Å bridged by a μ_2-oxo system, while in the other set by a longer distance of ca. 3.3 Å which is most probably bridged by a carboxylate group.

Thus, synthesis and characterization of manganese-hydroxy aromatic aldehyde and ketone complexes constitute an active area of research that promise to yield complexes that may act as effective models for the manganese cofactor of photosystem-II and for manganese superoxide dismutase. One ligand that finds much utility in this regard is salicylic acid (2-hydroxy benzoic acid,

---

* Corresponding author. Tel.: +91 03642722616; fax: +91 03642551634.
E-mail address: ramashraylal@rediffmail.com (R.A. Lal).

0020-1693/$ - see front matter © 2006 Published by Elsevier B.V.
doi:10.1016/j.ica.2004.11.044

H_2sal) whose phenolic and carboxylic acid functions are being used as convenient substitutes for the amino acid site groups of tyrosine and aspartic acid/glutamic acid, respectively [13].

2. Results and discussion

The crystal data showed that the general formula of the compound obtained is $[Mn_2(Hsal)_4(OH)_4]$. The compound is assumed to result from redox reaction in the presence of the reagent GS and pyridine.

The X-ray crystallographic data are listed in Table 1. Fractional coordinates are listed in Table 2 and selected bond distances and angles in Table 3.

The compound crystallizes in the monoclinic space group $P2_1/a$. The ORTEP diagram of compound is given in Fig. 1. There are two dimeric units in the unit cell (see Table 4, Fig. 2).

The complex is composed of two symmetry related pseudo six-coordinate Mn(IV) centers. Bidentate chelating and bridging $Hsal^-$ ($HOC_6H_4COO^-$) ligands asymmetrically coordinate each manganese.

Table 2
Atomic coordinates ($\times 10^4$) and equivalent isotropic displacement parameters ($Å^2 \times 10^3$) for the compound

	x	y	z	U_{eq}
C(1)	5926(6)	2979(4)	7398(4)	46(1)
C(2)	6677(7)	2529(4)	8222(4)	47(1)
C(3)	6808(9)	1416(4)	8343(4)	64(2)
C(4)	7520(11)	975(6)	9102(5)	82(2)
C(5)	8166(10)	1640(7)	9762(5)	83(2)
C(6)	8061(9)	2748(6)	9688(4)	73(2)
C(7)	7312(8)	3206(5)	8914(4)	57(2)
C(8)	4980(6)	3295(4)	4196(4)	45(1)
C(9)	5343(6)	2757(3)	3383(3)	40(1)
C(10)	5671(7)	3359(4)	2670(4)	49(1)
C(11)	6072(8)	2862(5)	1926(4)	60(2)
C(12)	6106(9)	1739(5)	1883(4)	66(2)
C(13)	5766(8)	1130(4)	2582(4)	57(2)
C(14)	5383(7)	1615(4)	3316(4)	46(1)
O(1)	5802(5)	4014(3)	7300(3)	60(1)
O(2)	5442(5)	2407(3)	6744(3)	57(1)
O(3)	4802(5)	2724(2)	4847(2)	51(1)
O(4)	5063(5)	976(2)	3996(3)	56(1)
O(5)	7909(5)	4038(3)	5754(3)	55(1)
O(6)	2286(5)	4125(3)	5974(3)	60(1)
O(7)	5101(5)	5695(3)	5756(3)	57(1)
O(8)	7233(7)	4296(4)	8866(3)	78(1)
Mn(1)	5071(1)	3971(1)	5875(1)	42(1)

U_{eq} is defined as one third of the trace of the orthogonalized U_{ij} tensor.

Table 1
Crystal data for $[Mn_2(Hsal)_4(OH)_4]$

Formula	$C_{28}H_{24}Mn_2O_{16}$
M	726.35
Crystal system	monoclinic
Space group	$P2_1/a$
Unit cell dimensions	
a (Å)	7.631(5)
b (Å)	12.320(5)
c (Å)	15.623(5)
β (°)	96.560(5)
V ($Å^3$)	1459.2(12)
Z	2
D_{calc} (mg/m^3)	1.653
$F(000)$	740
Crystal size (mm)	$0.3 \times 0.2 \times 0.2$
λ(Mo Kα) (Å)	0.71069
Number of collected reflections	2776
Number of unique reflections [R_{int}]	2562 [0.0463]
Data/restraints/parameters	2562/4/225
Absorption correction	ψ-scan
Maximum and minimum transmission	0.9921 and 0.5477
Refinement method	full-matrix least-squares on F^2
θ Range for data collection (°)	2.11–25.00
Limiting indices	$0 \leqslant h \leqslant 9$, $0 \leqslant k \leqslant 14$, $-18 \leqslant l \leqslant 18$
Completeness to $\theta = 5.00$	99.6%
Goodness-of-fit on F^2	0.947
Final R indices [$I > 2\sigma(I)$]	$R_1 = 0.0573$, $wR_2 = 0.1404$
R indices (all data)	$R_1 = 0.1079$, $wR_2 = 0.1592$
Extinction coefficient	0.0005(13)
Largest difference in peak and hole (e $Å^{-3}$)	0.508 and −0.569

The dimer consists of two Mn(IV) atoms which are bridged by carboxylato oxygen atoms (O_3, O_4, O_{3a} and O_{4a}) from salicylate group in syn–syn fashion of bidentate salicylate anion. Each Mn(IV) is further chelated by two oxygen atoms of carboxylato oxygen atoms of another bidentate salicylate anion. The six coordination around the metal center is completed by hydroxyl (OH^-) group that does not take part in coordination. The deposition of the ligands is such as to produce a dimer of C_2 symmetry. The Mn_2O_4 bridging unit is almost planar. The Mn(IV) ions are in a highly distorted octahedral environment with elongation of the three Mn–O bonds in the equatorial direction, i.e., Mn–O(1) = 2.234(4) Å, Mn–O(2) = 2.356(4) Å and Mn–O(3) = 2.215(3) Å except fourth Mn–O(4) = 2.133(3) Å which is shorter than the axial Mn–O(5) = 2.197(4) and Mn–O(6) = 2.157(4) Å. Although d^3 system is not subjected to Jahn–Teller distortion, even then the structure is highly distorted. This is most probably due to steric crowding around manganese centers due to bridged and chelated salicylato ligands.

Although angles at the metal subtended by trans-ligand atoms and a pair of angles subtended by cisoid ligands are reasonably close to the theoretical value for an octahedron (180° and 90°, respectively), yet pair of angles subtended by cisoid ligands differ widely from the theoretical value of 90°. Thus, the widely differing cisoid bond angles O_1–Mn–O_2 and O_3–Mn–O_4 are 56.27°

Table 3
Selected interatomic distances (Å) and bond angles (°) for the compound

Manganese environment			
O(1)–Mn(1)	2.234(4)	O(2)–Mn(1)	2.356(4)
O(3)–Mn(1)	2.215(3)	O(5)–Mn(1)	2.197(4)
O(6)–Mn(1)	2.157(4)	O(7)–Mn(1)	2.133(3)
C(1)–O(1)–Mn(1)	95.8(3)	C(1)–O(2)–Mn(1)	90.8(3)
C(8)–O(3)–Mn(1)	100.9(3)	C(14)–O(4)–H(4′)	110(2)
Mn(1)–O(5)–H(5′)	122(3)	Mn(1)–O(6)–H(6′)	124(3)
C(8)#1–O(7)–Mn(1)	170.5(4)	C(7)–O(8)–H(8′)	93(4)
O(7)–Mn(1)–O(6)	86.52(14)	O(7)–Mn(1)–O(5)	6.23(13)
O(6)–Mn(1)–O(5)	172.75(13)	O(7)–Mn(1)–O(3)	128.95(15)
O(6)–Mn(1)–O(3)	95.90(15)	O(5)–Mn(1)–O(3)	88.56(14)
O(7)–Mn(1)–O(1)	93.39(14)	O(6)–Mn(1)–O(1)	93.55(16)
O(5)–Mn(1)–O(1)	87.02(15)	O(3)–Mn(1)–O(1)	137.00(13)
O(7)–Mn(1)–O(2)	149.66(16)	O(6)–Mn(1)–O(2)	94.87(13)
O(5)–Mn(1)–O(2)	91.46(13)	O(3)–Mn(1)–O(2)	81.14(15)
O(1)–Mn(1)–O(2)	56.27(13)		
Salicylate chelate environment			
C(1)–O(2)	1.262(6)	C(1)–O(1)	1.286(6)
C(7)–O(8)	1.345(7)	C(1)–C(2)	1.458(8)
O(2)–C(1)–O(1)	116.6(5)		
Salicylate bridge environment			
C(8)–O(7)#1	1.248(5)	C(8)–O(3)	1.256(6)
C(8)–C(9)	1.486(7)	C(14)–O(4)	1.367(6)
O(7)#1–C(8)–O(3)	119.9(5)		

Symmetry transformations used to generate equivalent atoms: #1 $-x+1, -y+1, -z+1$.

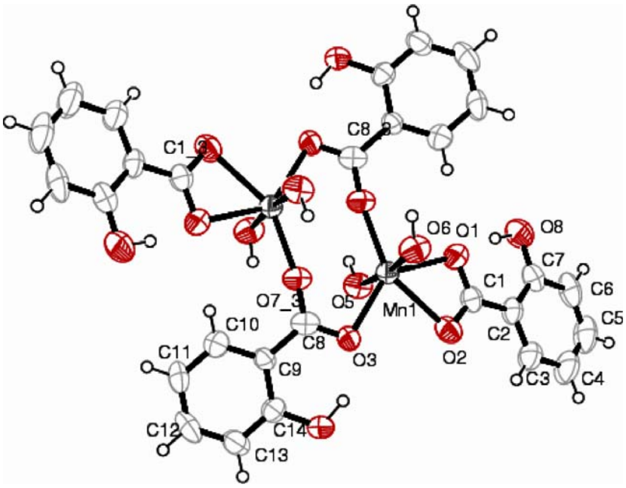

Fig. 1. ORTEP diagram of the compound.

Table 4
Hydrogen bonds for the compound (Å) and (°)

D–H···A	*d*(D–H)	*d*(H···A)	*d*(D···A)	∠(DHA)
O(5)–H(5′)···O(4)#2	0.9500(12)	1.899(7)	2.847(5)	175(5)
O(4)–H(4′)···O(3)	0.9500(11)	1.72(2)	2.550(5)	145(3)
O(6)–H(6′)···O(4)#3	0.9499(11)	1.973(13)	2.904(5)	166(5)
O(8)–H(8′)···O(1)	0.9500(11)	1.646(14)	2.585(7)	169(7)

Symmetry transformations used to generate equivalent atoms: #1 $-x+1, -y+1, -z+1$ #2 $-x+3/2, y+1/2, -z+1$ #3 $-x+1/2, y+1/2, -z+1$.

and 128.95°, while the reasonably close cisoid bond angles O_2–Mn–O_3 and O_1–Mn–O_4 are 81.14° and 93.39°. The larger deviations in cisoid bond angles are attributed to the asymmetry in the bridging and chelating region as clearly visible in Fig. 1.

For the chelating salicylato group, the Mn–O bond length is longer than those due to bridging salicylate group, arising from the steric crowding imposed by the neighboring bridging salicylate group. Thus, in the compound, the carboxylate functions of salicylate group ($Hsal^-$) form bond by means of bridging and chelating mode. The compound is quite stable in solid state due to the H-bonding between the phenolic-H atoms and chelating oxygen atom, coordinated hydroxyl-H atom and chelating oxygen atom.

A neutral manganese (IV) salicylate complex has been well characterized by Christou and coworkers [14], but to the best of our knowledge the present compound is the only dinuclear manganese (IV) salicylate complex containing bridging as well as chelating carboxylate functions of salicylato group. The structure may have some important implication in Lippard's 'Carboxylate Shift' phenomenon that relates to the structure, function and kinetics of carboxylate containing metalloproteins [15].

The compound is different from that of Christou and coworkers' [14] monomeric Mn^{IV} compound $[Mn(sal)_2(bipy)]$. The complex has no crystallographically imposed symmetry but does approach C_2 symmetry. Two salicylato groups and one bipyridyl group, salicylato ligand functions as a chelating bidentate ligand through phenoxide and one-carboxylato oxygen atoms, coordinate manganese atom. The phenoxide oxygen atoms are *cis* and carboxylato oxygen atoms are trans about the manganese.

2.1. Magnetic moment

The room temperature magnetic moment of a powdered sample of the compound ($\mu_B = 6.45$ BM at 25 °C) is slightly lower than the spin-only magnetic moment expected for a dimeric d^3 ion ($\mu_s = 6.90$ BM). This indicates either no interaction or a very weak interaction between metal ions in the solid state of the compound.

2.2. EPR spectra

The X-band EPR spectra of the complex were examined in polycrystalline phase (300 and 77 K) as well as in DMF glass (77 K). In the polycrystalline phase, two broad resonances are observed: a strong one near $g \cong 2$ and a weak one near $g \cong 4$. In the magnetically dilute glassy state, the ^{55}Mn hyperfine structure is well resolved for the resonance near $g \cong 2$.

Interestingly, ^{55}Mn hyperfine coupling constant for the $g \cong 2.0$ signal is equal to 75G which is close to the values observed for Mn (IV) complexes. Depending on

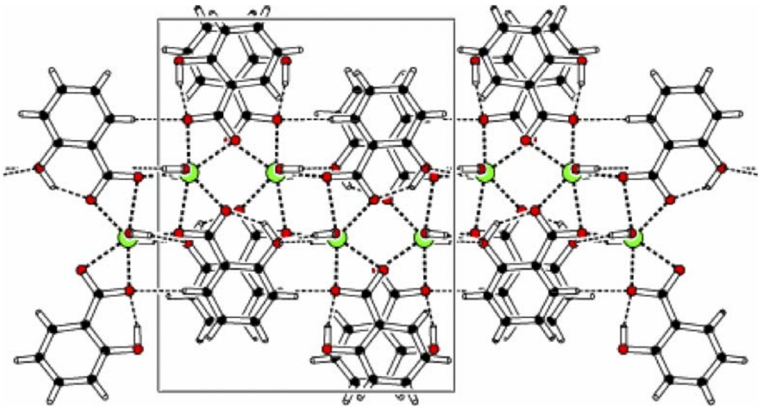

Fig. 2. ORTEP diagram of the unit cell.

the nature and extent of distortion of the ligand field from O_h symmetry, the frozen-solution EPR spectra of a $3d^3$ ion can assume different forms [16–18]. The form observed here (strong $g \sim 2$ and weak $g \sim 4$ resonances) is characteristic of small axial distortion: $2D \ll h\nu$, where D is the axial zero field splitting parameter and $h\nu$ is the microwave quantum (0.31 cm^{-1} at X-band). When D is small, rhombic splitting is necessarily very small, since $D/E \geqslant 3$, where E is the rhombic splitting parameter whereas the large distortion case $2D \gg h\nu$ occurs in a number of complexes [19–21], the $2D \ll h\nu$ situation for Mn(IV) has been documented in tris-(dithiocarbamate) [22] and in tris(thiohydroxamates) [18]. The spectral features observed in the present study (strong $g \sim 2$ and weak $g \sim 4$ resonances) are characteristic of small axial distortion, $2d \ll h\nu$. Interestingly, the ^{55}Mn hyperfine splitting constant for the $g \sim 2$ signal lies close to 78G for the known $2D \ll h\nu$ manganese (IV) species.

2.3. Infrared spectra

Infrared spectroscopy provides a means of distinguishing the mode of coordination of salicylato groups to the Mn^{IV} center. The IR spectrum of the compound has been interpreted by comparing the spectrum with that of sodium salicylate (NaHsal). The compound shows a split strong band in the region 3200–2300 cm^{-1}. The band in this region is attributed to ν(OH) of uncoordinated phenolic-OH group and coordinated hydroxyl group. The essential features of the band in this region indicate the presence of hydrogen bond involving phenolic-OH and coordinated OH groups, with carboxyl oxygen atom of coordinated carboxylato oxygen atoms.

The band observed at 1381 cm^{-1} in the free salicylate ion is attributed to ν_s(COO) vibration of carboxylato function, while that at 1593 cm^{-1} is attributed to ν_{as}(COO) vibrations of carboxylato function as well as phenyl ring [23]. In the complex, the ν_{as}(COO) and ν_s(COO) appear at 1600s and 1402s cm^{-1}, respectively.

2.4. Electronic spectra

The electronic spectrum of the compound in methanol shows a weak band in the visible region with strong absorbance in the ultraviolet region. Mn(IV) exhibits two absorption bands due to d–d electronic transitions (from the octahedral approximation $^4A_{2g} \rightarrow {}^4T_{2g}$ and $^4A_{2g} \rightarrow {}^4T_{1g}$) [24]. The compound shows a weak absorption band at $\lambda_{max} = 450$ nm ($\varepsilon_{max} = 0.71 \times 10^2$ l mol^{-1} cm^{-1}) and 530 nm ($\varepsilon_{max} = 0.332 \times 10^2$ l mol^{-1} cm^{-1}). These transitions are of low intensity and are attributed to arise due to $^4A_{2g} \rightarrow {}^4T_{2g}$ and $^4A_{2g} \rightarrow {}^4T_{1g}$ transitions, in excellent agreement with those reported for tris(thiohydroxamato)manganese(IV) [18] and the mononuclear tris(glucarate), tris(gluconato) and tris(sorbitolato)manganese (IV) complexes [25,26].

3. Experimental

3.1. Physical measurements

Infrared spectra were recorded on FT-IR Perkin–Elmer 983 spectrophotometer in the range 4000–450 cm^{-1} in KBr discs. The electronic spectra were recorded on a UV-2600 Double beam UV–Vis spectrophotometer. Room temperature magnetic susceptibility measurement was carried out on a vibrating sample magnetometer. Experimental magnetic susceptibility values have been corrected for diamagnetism by the procedures given by Figgis and Lewis [27] and Earnshaw [28]. The EPR spectra of the compound in powdered form and DMF solution at RT and LNT were recorded at X-band frequency on a Variance E-112X/2 band spectrometer, DPPH was used as an internal field marker. The molar conductance of the complex at 10^{-3} M dilution in methanol solution was measured on a Direct Reading conductivity meter-303 with a dip type conductivity cell at room temperature.

4. Synthesis of [$Mn_2(Hsal)_4(H_2O)_4$]

All manipulations were carried out under aerobic conditions. $Mn(OAc)_2 \cdot 4H_2O$, glycine, salicylaldehyde, salicylic acid, NaOH, pyridine and other solvents were E-Merk grade reagents, which were employed in the preparation of the complex as received. The reagent GS was prepared by refluxing glycine and salicylaldehyde in 1:1 molar ratio in 90% ethanol (30 mL) as follows:

Glycine (0.5 g, 6.67 mmol) in hot water (5 mL) was added to salicylaldehyde (6.72 mmol) in hot ethanol (20 mL). The resulting solution was refluxed for 1 h and then cooled. The precipitate was filtered and washed with ethanol. It was again dissolved in 90% ethanol – soln1.

Sodium salicylate was prepared by adding a solution of salicylic acid (1.18 g, 8.55 mmol) in methanol (20 mL) to a solution of NaOH (0.34 g, 8.5 mmol) in methanol – soln2.

To a solution of $Mn(OAc)_2 \cdot 4H_2O$ (0.70 g, 2.86 mmol) in methanol (25 mL), the reagent GS (soln1) was added drop wise accompanied by gentle stirring for 45 min at 40 °C. To the resulting solution, monosodium salicylate (soln2) was added drop wise with constant stirring and the reaction mixture was stirred for another 45 min at 40 °C. Then, pyridine (1.5 mL, 18.6 mmol) was added to the reaction medium dropwise with constant stirring and it was stirred for 45 min at 40 °C, followed by concentration to ca. 10 mL. On keeping the resulting deep reddish brown solution for 10 days at room temperature, the complex formed as deep brown colored crystals in 75% yield. The compound was recrystallized from methanol to yield deep brown colored block shaped monoclinic crystal. Yield: 80%. Anal. *Calc.* for [$Mn_2(Hsal)_4(OH)_4$]: Mn, 15.14; C, 46.26; H, 3.30. Found: Mn, 15.40; C, 47.73; H, 3.35%. It is soluble in EtOH, MeOH, CH_3CN, DMF, and DMSO and insoluble in diethyl ether, benzene, chloroform, dichloromethane and other common organic solvents.

IR (KBr): ν/cm^{-1}(OH) 3200–2300sbr band with splitting into several bands, $\nu_{as}(CO_2)$ 1600s and $\nu_s(CO_2)$ 1348s. λ_M (in MeOH) = 26.3 $\text{ohm}^{-1}\,\text{cm}^2\,\text{mol}^{-1}$. Electronic spectrum ($CH_3OH$) [$\lambda_{max}$, nm ($\varepsilon/Mn^{IV}$, $\text{l mol}^{-1}\,\text{cm}^{-1}$)]: 450 ($0.71 \times 10^2$) and 530 ($0.332 \times 10^2$).

4.1. X-ray crystallography

Suitable crystals of [$Mn_2(Hsal)_4(OH)_4$] were obtained as described above. Crystals for single crystal X-ray diffraction study were chosen and mounted on glass fibers and transferred to an Enraf-Nonius XCAD4 diffractometer equipped with a graphite-monochromated Mo Kα X-ray source ($\lambda = 0.71069$ Å). The unit cell parameters were determined using the method of short vectors followed by least-squares refinement of 25 well-centered reflections. Data were collected at 293 K using $\omega < 2\theta$ scan technique. Intensities of two standard reflections monitored every 1 h showed 0% variation during the data collection time. An empirical absorption correction [29] based on ψ-scans was also applied for the compound. All the calculations were performed using a software package 'XCAD4 (WINGX)' adapted on a Micro VAX 3100 computer.

Space groups were assigned on the basis of systematic absences and crystallographic E-statistics. Atomic scattering factors for neutral atoms Mn, O, C and H were taken from [30]. Anomalous dispersion was taken into account. The structure was solved by using 'SIR92 (WINGX)' [31] and refined by using 'SHELXL-97 (Sheldrick, 1997)' [32]. The molecular graphics was solved by using the direct methods program 'ORTEP3' [33] included in WINGX [34] version. Atomic coordinates were refined using anisotropic thermal parameters for all non-hydrogen atoms. Hydrogen atoms are located on a difference Fourier map.

5. Supplementary data

Tables of anisotropic displacement parameters, all bond lengths and angles for the compound (5 pages); listing of calculated and observed structure factors (7 pages) in CIF form.

Acknowledgements

The authors are thankful to the authorities of Tripura University, Suryamaninagar 799130, Tripura, India and North-Eastern Hill University, Shillong 793022, Meghalaya, India for providing facilities for carrying out this work. They thank the Head, Regional Sophisticated Instrumentation Centre, IIT, Madras, Chennai, India for Crystallographic and EPR spectral studies and the Head, Department of Inorganic Chemistry, Indian Association for Cultivation of Science, Jadavpur, Kolkata 32 for magnetic susceptibility data.

References

[1] M.L. Ludwig, K.A. Pattridge, W.C. Stalings, Manganese in Metabolism and Enzyme Function, Academic Press, New York, 1986 (Chapter 21).

[2] W.F. Beyer, I. Findovich, Ref. [1], Chapter 12, p. 193.

[3] Photosynthetic Water Oxidation: J. Nugeni (Ed.), Special Dedicated Issue: Biochim. Biophys. Acta: Bioenergy, 1503 (2001) pp. 1–259.

[4] V.L. Pecororo, Manganese Redox Enzymes, VCH Publishers, New York, 1992.

[5] J.E. Penner-Hahn, Struct. Bonding 90 (1998) 1.

[6] V.K. Yachandra, K. Sauer, M.P. Klein, Chem. Rev. 96 (1996) 2927.

[7] W. Ruttinger, G.C. Dismukes, Chem. Rev. 97 (1997) 1.

[8] C. Tommos, G.T. Babcock, Acc. Chem. Res. 31 (1998) 18.

[9] G.L. Lawrence, D.T. Sawyer, Coord. Chem. Rev. 27 (1978) 173.

[10] M.R. Bermejo, A. Gercia-Deibe, J. Sanmartin, A. Sousa, N. Aurangzeb, C.E. Hulme, C.A. McAuliffe, R.G. Pritchard, M. Watkinson, J. Chem. Soc., Chem. Commun. (1994) 645.

[11] V.K. Yachandra, V.J. DeRose, M.J. Latimer, I. Mukerji, K. Sauer, M.P. Klein, Science 260 (1993) 675.

[12] J.H. Robblee, J. Messinger, R.M. Cinco, K.L. McFarlane, C. Fernadez, S.A. Pizzaro, K. Sauer, V.K. Yachandra, J. Am. Chem. Soc. 124 (2002) 7459.

[13] J.B. Vincent, K. Folting, J.C. Huffman, G. Christou, Inorg. Chem. 25 (1986) 996.

[14] P.S. Pavacik, J.C. Huffman, G. Christou, J. Chem. Soc., Chem. Commun. (1986) 43.

[15] R.L. Rardin, A. Bino, P. Poganiuch, W.B. Tolman, S. Liu, S.J. Lippard, Angew. Chem., Int. Ed. Engl. 29 (1990) 812.

[16] J.C. Hempel, L.O. Morgan, W.B. Lewis, Inorg. Chem. 9 (1970) 2064.K.

[17] E. Pedersen, H. Toftlund, Inorg. Chem. 13 (1974) 1603.

[18] S. Pal, P. Ghosh, A. Chakravorty, Inorg. Chem. 24 (1985) 3704.

[19] S.K. Chandra, P. Basu, D. Ray, S. Pal, A. Chakraborty, Inorg. Chem. 29 (1990) 2423.

[20] D.T. Richens, D.T. Sawyer, J. Am. Chem. Soc. 101 (1979) 3681.

[21] M.W. Lynch, D.N. Hendrickson, B.J. Fitzgerald, C.G. Pierpont, J. Am. Chem. Soc. 106 (1984) 2041.

[22] K.L. Brown, R.M. Golding, P.C. Healy, K.J. Jessop, W.C. Tennant, Aust. J. Chem. 27 (1974) 2075.

[23] Nakamoto, Infrared and Raman Spectra of Inorganic and Coordination Compounds, third ed., Wiley, New York, 1978, p. 232.

[24] A.B.P. Lever, Inorganic Electronic Spectroscopy, second ed., Elsevier, Amsterdam, 1984, p. 431.

[25] D.T. Richens, C.G. Smith, D.T. Sawyer, Inorg. Chem. 18 (1979) 706.

[26] M.E. Bodini, L.A. Willis, T.L. Riechel, D.T. Sawyer, Inorg. Chem. 15 (1976) 1538.

[27] B.N. Figgis, J. Lewis, in: J. Lewis, R.G. Wilkins (Eds.), Mordern Coordination Chemistry, Interscience, New York (1960) p. 403.

[28] A. Earnshaw, Introduction to Magnetochemistry, Academic Press, London, 1968, p. 35.

[29] C.T. North, D.C. Phillips, F.S. Mathews, Acta Crystallogr. A24 (1968) 351.

[30] D.T. Cromer, J.T. Waber, International Table for X-ray Crystallography, vol. IV, Kynoch Press, Birmingham, UK, 1974, Table 2.2B.

[31] A. Altomare, G. Cascarano, C. Giacovazzo, M.C. Burla, G. Polidori, N.J. Camalli, Appl. Crystallogr. 24 (1994) 435.

[32] SHELXL-97: G.M. Sheldrick, A Computer Program for Refinement of Crystal Structures, University of Gottingen.

[33] M.N. Burnett, C.K. Johnson, ORTEPIII: Oak Ridge Thermal Ellipsoid Plot Program for Crystal Structure Illustrations. Oak Ridge National Laboratory Report ORNL-6895, Oak Ridge National Laboratory, TN, 1996.

[34] L.J. Farrugia, J Appl. Crystallogr. 32 (1999) 837.